Revolutionizing Electric Vehicle Charging: The Interleaved Buck Converter Approach

Fifi Hesty Sholihah[1], Syechu Dwitya Nugraha [2], Era Purwanto [3]

[1,2,3] Politeknik Elektronika Negeri Surabaya
fifi@pens.ac.id

Abstract. The rise of electric vehicles (EVs) has transformed the automotive industry, offering an eco-friendly mode of transportation. However, the success of EVs depends on efficient and reliable battery charging systems. With the global shift towards electric mobility, the demand for advanced charging tech is clear. DC-DC converters play a vital role, adapting DC power source voltage for various devices, from smartphones to EVs, crucial for fast charging. EV chargers have evolved from basic DC-DC designs, with isolated and non-isolated converters being prominent. Non-isolated converters, favored due to lower power needs, rely on traditional structures like buck-boost, Cuk, and SEPIC. This paper explores the interleaved buck converter's integration into EV charging, highlighting its efficiency and reliability. It's ideal for both on-board and off-board chargers, ensuring consistent output voltage and high efficiency across SOC levels, vital for efficient battery charging in the evolving electric mobility landscape.

Keywords: Charging; Interleaved Buck Converter, fast charging

1 Introduction

The evolution of electric vehicles (EVs) has reshaped the automotive industry by offering a sustainable and environmentally friendly mode of transportation. However, the practicality and adoption of EVs are intricately tied to the efficiency, speed, and reliability of their battery charging systems. As the global transition towards electric mobility accelerates, the need for advanced charging technologies becomes increasingly apparent.

DC-DC power converters are integral components within the realm of advanced charging technologies, facilitating the efficient and controlled transfer of electrical energy between various devices and systems [1]. These converters excel in adapting the voltage levels of direct current (DC) power sources to meet the specific demands of the target device or application, whether it's a smartphone, laptop, or electric vehicle.

M. U. H. Al Rasyid and M. R. Mufid (eds.), *Proceedings of the International Conference on Applied Science and Technology on Engineering Science 2023 (iCAST-ES 2023)*, Advances in Engineering Research 230,
https://doi.org/10.2991/978-94-6463-364-1_107

Their role is particularly crucial in fast charging scenarios, where voltage regulation and current management are paramount to optimize charging speed while safeguarding against overcharging or overheating. In the context of advanced charging technologies, DC-DC power converters serve as adaptable workhorses, ensuring that the right amount of power is delivered to devices, thus expediting the charging process, enhancing energy efficiency, and maintaining the integrity of the charged equipment [2].

EV chargers have developed from basic DC-DC converter designs over time. There are two types of DC-DC Converter, isolated and non-isolated DC-DC Converter. Isolated DC-DC converters achieve electrical isolation between the input and output sections through the utilization of a high-frequency transformer [3]. These converters come in various configurations, which can be categorized as single-switch designs (such as Flyback and forward converters) and multi-switch designs (like Push-pull, half-bridge, and full bridge).

Isolated DC-DC converters come with certain drawbacks, including issues like transformer core saturation and primary-side switch current stresses caused by discontinuous mode operation. Additionally, half-bridge converters might be compelled to function at lower switching frequencies when dealing with low input voltage situations, which can result in elevated current fluctuations.

Given the relatively low power needed for charging EVs, non-isolated converter designs continue to be favored by researchers. In the context of DC charging, non-isolated converters that have been reported predominantly rely on traditional DC-DC converter structures like buck-boost, Cuk, and SEPIC, which is evident in on-board non-isolated chargers [4].

Several types of DC-DC converters are employed for Electric Vehicle (EV) charging, with two prominent examples being the boost converter and the full-bridge converter. The boost converter is recognized for its reliance on relatively straightforward switching techniques, making it an attractive choice for certain applications [5]. However, it does come with a trade-off in terms of lower efficiency, as it may experience more power losses during the conversion process.

On the other hand, the full-bridge converter offers a different set of advantages. This converter is frequently favored in the context of bidirectional charging systems, which allow power to flow both into and out of the EV's battery [6].

This research paper delves comprehensively into the integration of the interleaved buck converter within Electric Vehicle (EV) charging systems. It focuses on the intricate details of how this converter type is applied to EV charging, including design considerations, operational principles, and performance characteristics.

The Interleaved Buck Converter is a favorable choice for advanced EV charging technologies due to its efficiency, scalability, fast charging capabilities, and reliability. The interleaved buck converter is primarily suitable for both on-board and off-board chargers, especially in high-power, fast-charging stations.

2 Interleaved Buck Converter for Advanced EV Charging

2.1 DC-DC Interleaved Buck Converter (IBC)

The DC-DC Interleaved Buck Converter (IBC) is a converter that operates using interleaved (alternating) methods and is used to convert electrical voltage from higher levels to lower levels within a system. IBC is often used in various applications, including electric vehicle (EV) charging, and they have advantages in terms of efficiency and reducing heat generated during the conversion process [7].

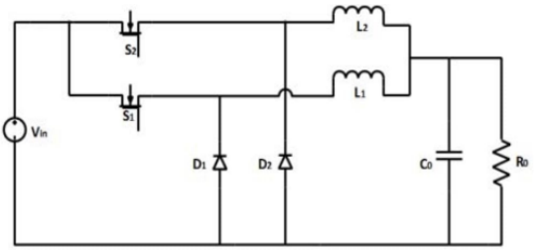

Fig. 1. Interleaved Buck Converter Circuit

The IBC circuit, as shown in Figure 1, consists of a DC input voltage, 2 switches which can be either IGBTs or MOSFETs, 2 diodes, 2 inductors, a capacitor, and a load on the output side [8]. The switches (MOSFET/IGBT) in the IBC circuit operate in an on-and-off manner. Therefore, the operational principle of the IBC circuit is analyzed when the switches are ON and OFF. In the IBC circuit, there are two switches that operate alternately. Mode 1 occurs when Switch 1 is ON, as depicted in Figure 2(a). Conversely, Mode 2 is activated when Switch 2 is turned ON, as illustrated in Figure 2(b).

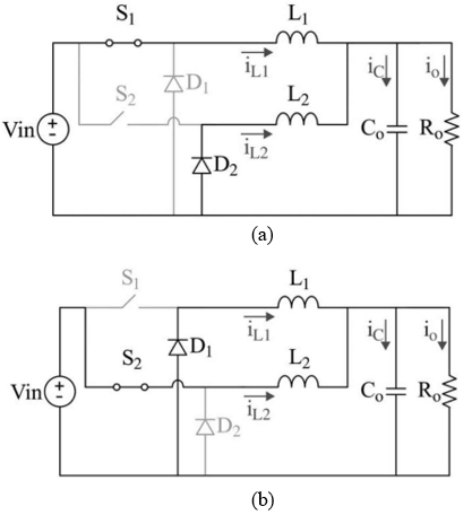

Fig. 2. Interleaved Buck Converter Circuit (a) mode 1; (b) mode 2

Mode 1, as depicted in Figure 2(a), occurs when S1 is in the ON position. In this mode, current flows through inductor L1, initiating the charging process of the inductor. Diode D1 is in a reversed bias condition, while diode D2 is in a forward bias condition. Current flows through inductor L2 via diode D2. By analyzing the Mode 1 circuit, the following equation is obtained:

$$VL1 = Vs - Vo = L\frac{diL}{d(t)} \quad (1)$$

Thus, (2)

$$\Delta iL1(charged) = \frac{Vs-Vo}{L1} \; x \; \Delta \text{ton}$$

$$\Delta iL1 = \frac{Vs - Vo}{L1} \; x \; DT \quad (3)$$

$$VL2 = -Vo = L\frac{diL}{d(t)} \quad (4)$$

$$L2 \; x \frac{\Delta iL2}{\Delta t \; off} = -Vo \quad (5)$$

$$\Delta iL2(discharged) = \frac{-Vo}{L2} (1\text{-}D) \; T \quad (6)$$

Mode 2, as illustrated in Figure 2(b), occurs when S2 is in the ON position. In this mode, current flows through inductor L2, initiating the charging process of the inductor. Diode D2 is in a reversed bias condition, while diode D1 is in a forward bias condition. Current flows through inductor L1 via diode D1. By analyzing the Mode 1 circuit, the following equation is obtained:

$$VL2 = Vs - Vo = L\frac{diL}{d(t)} \quad (7)$$

Thus, (8)

$$\Delta iL2(charge) = \frac{Vs-Vo}{L1} \; x \; \Delta \text{ton}$$

$$\Delta iL2 = \frac{Vs - Vo}{L1} \; x \; DT \quad (9)$$

$$VL1 = -Vo = L\frac{diL}{d(t)} \quad (10)$$

$$L1 \; x \frac{\Delta iL2}{\Delta t \; off} = -Vo \quad (11)$$

$$\Delta iL1(discharged) = \frac{-Vo}{L2} (1\text{-}D) \; T \quad (12)$$

2.2 Battery Charging Method

A. Constant Voltage

This method is a charging process carried out with a constant voltage from the beginning to the end of the charging process, with the charging current gradually decreasing according to the battery's capacity [9]. At the start of the charging process, a relatively high current is provided, and then, after some time, the current is reduced. Finally, the charging process is terminated when the current can no longer flow.

To maintain a constant voltage, adjustments are made in the duty cycle. The lower the output voltage compared to the set point, the higher the percentage of the duty cycle. Conversely, if the output voltage is significantly higher than the set point, the duty cycle percentage decreases. The advantage of charging with a constant voltage is its ability to charge batteries with different capacities and different discharge rates. The high charging current at the beginning of the charging process has a short duration and will not damage the cells. At the end of the charging process, because the battery voltage is nearly equal to the supply voltage, the charging current decreases to almost zero.

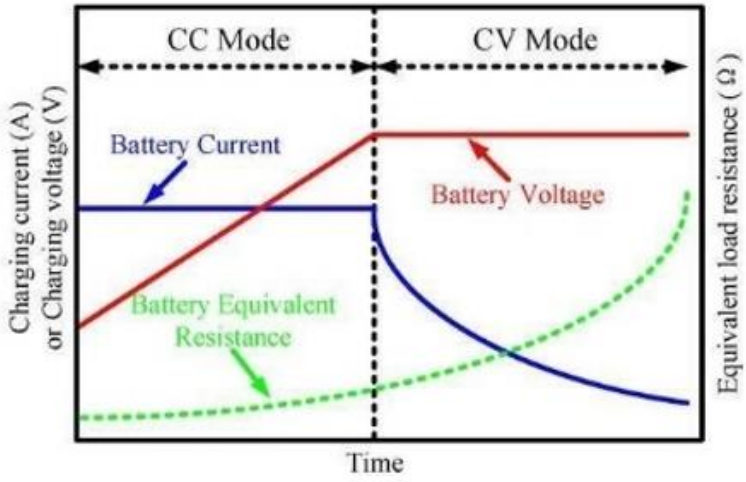

Fig. 3. CC-CV (Constant Current – Constant Voltage) Battery Charging

B. Floating Charge

The Floating Charge Charging Method aims to keep the battery in a full state, where the battery neither discharges nor receives electric current when it reaches the floating voltage, and the battery remains connected to the charger circuit. This charging method maintains the battery's condition stable during the charging process, without the worry of overcharging, while also keeping the battery full to reduce the self-discharge effect of the battery.

3 Methodology

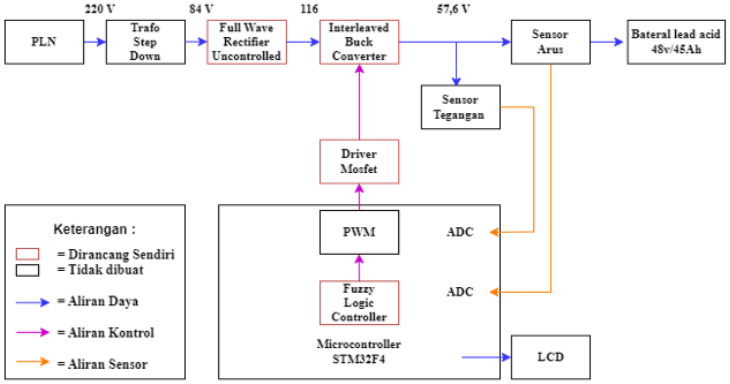

Fig. 4. System Block Diagram

This system utilizes a 48V/45Ah lead-acid battery as the voltage source and also incorporates several sensors. The system design relies on the ARM STM32F407VGTX microcontroller as the central controller. The LCD serves to display the battery charging status, as well as the magnitude of voltage and current readings obtained from current and voltage sensors. Within this system, battery charging control is achieved through an Interleaved Buck Converter, which exclusively accepts DC voltage. Consequently, the voltage originating from the utility grid (PLN) must be rectified before entering the Interleaved Buck Converter. Subsequently, the voltage output produced by the Interleaved Buck Converter is measured by a voltage sensor, and if this voltage is low or unstable, it can be adjusted using PWM via the ARM STM32F407VG microcontroller employing Fuzzy control methods. This device employs the step charging method CV-floating charge, where the voltage is kept constant, and when the current falls below 4 amperes, the floating charge method is utilized to maintain the battery terminal voltage value.

The full-wave rectifier in this system functions as a converter of AC voltage into DC voltage to be fed into the IBC circuit. The AC voltage to be rectified is first reduced using a transformer. The voltage reduction is carried out from 220 V to 84 V. This 84 V AC voltage is rectified into 113 V using a full-wave rectifier. This full-wave rectifier also employs a capacitor filter with a capacity of 4000 uF.

The voltage sensor used in this device operates based on the voltage divider principle, which involves utilizing two resistors to modify the voltage to be detected according to the voltage range that can be read by the Analog to Digital Converter (ADC) in the STM32F407VG microcontroller. The voltage range processed into the ADC is 0 - 3 volts, and in this planning, a 3-volt output voltage is used with an input voltage of 60 volts. For the sensor reading, which is 60 volts, the sensor design is the same. The design of the voltage divider sensor is as follows:

$$\text{Vadc} = \frac{R2}{(R1+R2)}\ x\ Vin \qquad (13)$$

The value of resistor R1 is determined to be 33 kΩ. Thus, according to equation 13, the value of resistor R2 is 2 kΩ.

The current sensor used in this system is the ACS712 module. This module requires a 5 Volt power source, and its readings will be converted by the STM32F407VG microcontroller using an Analog to Digital Converter (ADC). In the planning of this system, the ACS712 module with a current specification of 20 A is used.

The IBC circuit is designed based on Table I with a design target to achieve a ripple current value of 20% and a voltage value of 0.2%. The design of the IBC circuit is calculated based on equations derived from the circuit analysis in modes 1 and 2. In the IBC circuit, snubber components have been added to protect the switch. The snubber components consist of a diode, resistor, and capacitor, with a snubber resistor value of 4700 ohms and a snubber capacitor value of 1 nF.

TABLE I. IBC PARAMETER

Input Voltage	113 V
Output Voltage	57.6 V
Output Curent	6.75 A
Switching Frequency	40 kHz
Resistor	8.53 ohm
Inductor L1 dan L2	1306 uH
Capacitor	820 uF

The battery used is a lead-acid type with a capacity of 48V/45 Ah. Based on the specifications of this battery, the charging voltage applied is approximately 57.6 V, calculated as 120% of the battery's rated voltage. Additionally, the battery charging current has been planned with a value of 6.75 A, in accordance with the system's requirements to ensure the battery remains efficient and adequately charged.

4 Result and Discussion

Testing is conducted sequentially for each component before the integration process. The focus of this paper is the testing of the integrated system, and it will describe several testing schemes that have been conducted, namely:

1. Testing the simulation system using MATLAB Simulink

   In this stage, the paper will discuss testing the integrated system using MATLAB Simulink simulation tools.

2. Interleaved Buck Converter Testing

   Additionally, the paper will encompass the testing of the Interleaved Buck Converter component.

3. Testing the experimental/hardware system

   Additionally, the paper will also discuss testing the system through experiments/hardware testing.

4.1 Simulation System using Simulink Matlab

The system testing with SOC Variation is conducted by executing MATLAB software in a closed-loop circuit that uses a battery load. The battery specifications used in the simulation are a 48V 45Ah lead-acid battery, with SOC varying from 30% to 90%. The voltage source for the IBC is derived from the output of a rectifier that previously received input from an AC voltage source. The output voltage generated by the rectifier serves as a constant input voltage for the IBC, measuring 117 volts.

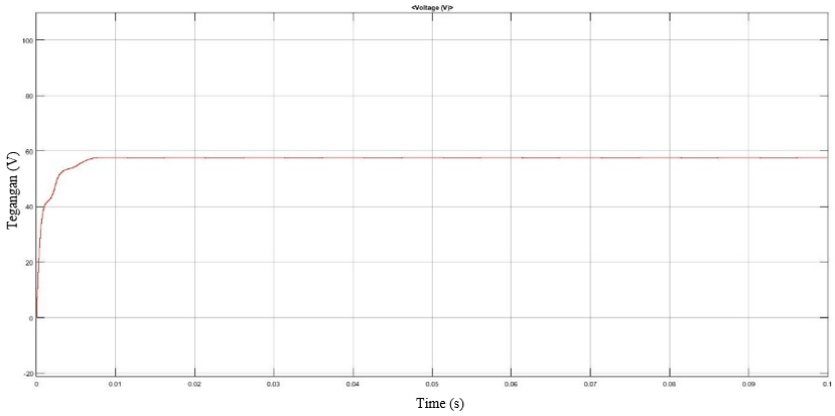

Fig. 5. Output Voltage

In Figure 5, the output response of the charging system when the SOC reaches 80% with a runtime of 1 second is shown. Under these conditions, the generated output voltage remains constant at 57.6 V, in accordance with the method used, which is Constant Voltage. Additionally, when using the floating charging method, the generated output voltage also remains constant at 54.5 V. Table II below provides the simulation results with SOC data sampling.

TABLE II. DATA OF CLOSE LOOP TESTING WITH SOC VARIATION

SOC(%)	Vin(V)	Vout(V)	Iout(A)
30	117	57,55	14,29
40	117	57,59	11,19
50	117	57,61	9,13
60	117	57,62	7,65
70	117	57,64	6,53
80	117	57,64	5,66
90	117	54,6	4,96
93	117	54,5	3,75
95	117	54,5	1,98
98	117	54,5	0,86

Table II and Figure 6 present data regarding input voltage, output voltage, and output current. The data clearly demonstrates a trend where, as the SOC value increases, the output current decreases. For instance, at SOC 30%, the recorded output current is 14.29 A.

Notably, the output voltage remains consistently within the range of 57.5 V to 57.6 V. Furthermore, under the floating condition, the output values exhibit a stable pattern, ranging between 54.6 volts and 54.5 volts, aligning perfectly with the expected setpoint. Figure 4.14 provides a visual representation of the successful maintenance of constant output voltage in both the CV and Floating methods.

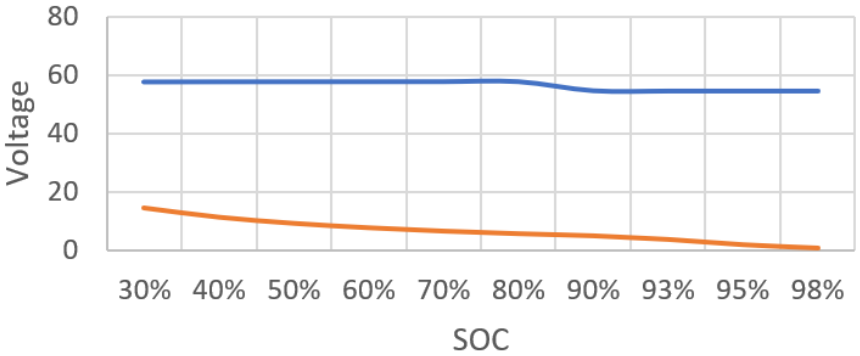

Fig. 6. The Graph of the Relationship Between SOC, Voltage, and Current

4.2 Interleaved Buck Converter Testing

The converter testing is conducted to assess its functionality and reliability according to the design power. There are two variations in converter testing, namely with a fixed duty cycle and a variable duty cycle.

The test results are presented in Table III and Table IV. In these tables, it is explained that with a fixed duty cycle of 51%, the converter's output voltage aligns with the design calculations, achieving an average efficiency of 96.54%. Meanwhile, during the testing with varying duty cycles, the resulting average efficiency is approximately 95.56%.

TABLE III. IBC TESTING WITH FIXED DUTY CYCLE

Duty (%)	Vin (V)	Vout (V)	Iin (A)	Iout (A)	Pin (Watt)	Pout (Watt)	Efficiency (%)
51	20	9,93	0,14	0,27	2,8	2,68	95,75
51	40	20,02	0,27	0,52	10,8	10,41	96,39
51	60	30,12	0,41	0,78	24,6	23,49	95,50
51	80	40,26	0,52	1,02	41,6	41,07	98,71
51	100	50,5	0,65	1,24	65	62,62	96,34
51	116	58,4	0,73	1,4	84,68	81,76	96,55
Average Efficiency							96,54

TABLE IV. IBC TESTING WITH VARIABLE DUTY CYCLE

Duty (%)	Vin (V)	Iin (A)	Vo (V)	Iout (A)	Pin (Watt)	Pout (Watt)	Efficiency (%)
41	116	0,46	46,7	1,1	53,36	51,37	96,27
51	116	0,73	58,4	1,4	84,68	81,76	96,55
61	116	1,06	69,9	1,69	122,96	118,131	96,07
71	116	1,53	81,4	1,98	177,48	161,172	90,81
81	116	1,91	92,9	2,34	221,56	217,386	98,12
Average Efficiency							95,56

The comprehensive converter testing, encompassing both fixed and variable duty cycle scenarios, demonstrates that the converter consistently meets design specifications. It maintains precise output voltage alignment with design calculations and achieves remarkable average efficiency levels, ensuring its functionality and reliability for diverse operational conditions.

4.3 Testing the experimental/hardware system

In addition to the simulation-based testing discussed earlier, this paper will provide an in-depth exploration of the practical aspects of testing the integrated system using real-world hardware experiments. These experiments will involve physically implementing and assessing the system's performance, providing valuable insights into its real-world functionality and reliability.

Fig. 7. Documentation of System Testing

The system testing results are shown in Figure 7. In this test, it was found that the initial battery voltage condition was 47.25 Volts (SOC 30%), while the final condition was 50.82 Volts (SOC 98%). Below is the closed-loop testing table. Table V below indicates that the charging test begins from SOC 30% to 98%.

TABLE V. IBC TESTING WITH VARIABLE DUTY CYCLE

Vbatt (V)	SOC (%)	Vin (V)	Vout (V)	Iin (A)	Iout (A)	Efficiency (%)
47,25	30	64	56,7	6,01	6,24	91,98
47,87	40	64	56,7	5,76	5,96	91,67
48,43	50	64	56,6	5,42	5,71	93,17
48,99	60	64	56,8	5,19	5,42	92,68
49,51	70	64	56,9	4,97	5,07	90,70
50,02	80	64	57,1	4,42	4,67	94,27
50,5	90	64	57,6	3,89	4,02	93,01
50,61	93	64	54,4	3,21	3,5	92,68
50,72	95	64	54,5	3,02	3,35	94,46
50,82	98	64	54,4	2,77	2,99	91,75

From the table above we can conclude that as the SOC increases from 30% to 98%, the battery voltage (Vbatt) also increases from 47.25 V to 50.82 V. This is expected behavior as a higher SOC corresponds to a higher battery voltage. The input voltage (Vin) remains constant at 64 V throughout the tests. This suggests that the input voltage source is stable and not affected by changes in SOC. The output voltage (Vout) remains relatively stable within the range of 54.4 V to 57.6 V across different SOC levels. However, there's a slight drop in voltage at SOC 93%, but it stabilizes afterward. This indicates that the system maintains a consistent output voltage for most SOC levels.

The input current (Iin) decreases as the SOC increases. This is because, at higher SOC levels, the battery requires less charging current. The input current varies from 6.01 A at SOC 30% to 2.77 A at SOC 98%. Similar to input current, the output current (Iout) decreases as SOC increases. At SOC 30%, it's 6.24 A, and at SOC 98%, it's 2.99 A. This behavior aligns with typical charging profiles, where the charging current decreases as the battery approaches full capacity.

Efficiency, expressed as a percentage, ranges from approximately 90.7% to 94.46%. It's worth noting that the efficiency is relatively high across SOC levels, indicating that the charging system is operating efficiently. The highest efficiency is observed at SOC 95%.

5 Conclusion

- The battery voltage increases proportionally with SOC, demonstrating a consistent and predictable relationship between SOC and battery voltage.
- The input voltage (Vin) remains stable at 64 V across different SOC levels, indicating that the charging system is not influenced by variations in the input voltage source.
- The output voltage (Vout) exhibits remarkable consistency, ranging from 54.4 V to 57.6 V across SOC levels. Although there is a minor dip in voltage at SOC 93%, it

quickly stabilizes, showcasing the system's ability to maintain a steady output voltage.

- As SOC increases, the input current (Iin) decreases, aligning with the expected behavior of battery charging. The system efficiently adjusts the charging current to match the battery's requirements.
- The charging system consistently demonstrates good efficiency, with values ranging from approximately 90.7% to 94.46% across SOC levels. This signifies that the system operates efficiently, even at different states of charge, with the highest efficiency observed at SOC 95%.

These findings indicate that the battery charging system effectively manages input and output parameters, maintaining a stable output voltage and achieving high efficiency across a wide range of SOC levels. This performance is crucial for ensuring the reliable and efficient charging of batteries in various applications.

References

1. M. A. H. Rafi and J. Bauman, "A Comprehensive Review of DC Fast-Charging Stations With Energy Storage: Architectures, Power Converters, and Analysis," in IEEE Transactions on Transportation Electrification, vol. 7, no. 2, pp. 345-368, June 2021, doi: 10.1109/TTE.2020.3015743.
2. Sutar, Amol & Patil, Mahadev. (2022). On the Advancements in DC Fast Charging Power Converters Technologies for Electric Vehicle. I.S. Jacobs and C.P. Bean, “Fine particles, thin films and exchange anisotropy,” in Magnetism, vol. III, G.T. Rado and H. Suhl, Eds. New York: Academic, 1963, pp. 271-350.
3. A. Mehdipour and S. Farhangi, "Comparison of three isolated bi-directional DC/DC converter topologies for a backup photovoltaic application," 2011 2nd International Conference on Electric Power and Energy Conversion Systems (EPECS), Sharjah, United Arab Emirates, 2011, pp. 1-5, doi: 10.1109/EPECS.2011.6126822.
4. Jeremy, L. & Ooi, Chia Ai & Teh, Jiashen. (2020). Non-isolated conventional DC-DC converter comparison for a photovoltaic system: A review. Journal of Renewable and Sustainable Energy. 12. 013502. 10.1063/1.5095811.
5. Ravyts, S.; Van De Sande, W.; Vecchia, M.D.; Broeck, G.V.d.; Duraij, M.; Martinez, W.; Daenen, M.; Driesen, J. Practical Considerations for Designing Reliable DC/DC Converters, Applied to a BIPV Case. Energies 2020, 13, 834. https://doi.org/10.3390/en13040834
6. Zhou, K.; Wu, Y.; Wu, X.; Sun, Y.; Teng, D.; Liu, Y. Research and Development Review of Power Converter Topologies and Control Technology for Electric Vehicle Fast-Charging Systems. Electronics 2023, 12, 1581. https://doi.org/10.3390/electronics12071581
7. A. Garg and M. Das, "High Efficiency Three Phase Interleaved Buck Converter for Fast Charging of EV," 2021 1st International Conference on Power Electronics and Energy (ICPEE), Bhubaneswar, India, 2021, pp. 1-5, doi: 10.1109/ICPEE50452.2021.9358486.
8. A. Garg and M. Das, "High Efficiency Three Phase Interleaved Buck Converter for Fast Charging of EV," 2021 1st International Conference on Power Electronics and Energy (ICPEE), Bhubaneswar, India, 2021, pp. 1-5, doi: 10.1109/ICPEE50452.2021.9358486.
9. Blinov, A.; Verbytskyi, I.; Zinchenko, D.; Vinnikov, D.; Galkin, I. Modular Battery Charger for Light Electric Vehicles. Energies 2020, 13, 774. https://doi.org/10.3390/en13040774